

# Granular activated algae for wastewater treatment

O. Tiron, C. Bumbac, I. V. Patroescu, V. R. Badescu and C. Postolache

## ABSTRACT

The study used activated algae granules for low-strength wastewater treatment in sequential batch mode. Each treatment cycle was conducted within 24 h in a bioreactor exposed to  $235 \mu\text{mol}/\text{m}^2/\text{s}$  light intensity. Wastewater treatment was performed mostly in aerobic conditions, oxygen being provided by microalgae. High removal efficiency of chemical oxygen demand (COD) was achieved (86–98%) in the first hours of the reaction phase, during which the indicator's removal rate was  $17.4 \pm 3.9 \text{ mg O}_2/\text{g h}$ ;  $\text{NH}_4^+$  was removed during organic matter degradation processes with a rate of  $1.8 \pm 0.6 \text{ mg/g h}$ . After almost complete COD removal, the  $\text{NH}_4^+$  remaining in the liquor was removed through nitrification processes promoted by the increase of the liquor's oxygen saturation ( $\text{O}_2\%$ ), the transformation rate of  $\text{NH}_4^+$  into  $\text{NO}_3^-$  increasing from  $0.14 \pm 0.05$  to  $1.5 \pm 0.4 \text{ mg NH}_4^+/\text{g h}$ , along with an  $\text{O}_2\%$  increase. A wide removal efficiency was achieved in the case of  $\text{PO}_4^{3-}$  (11–85%), with the indicator's removal rate being  $1.3 \pm 0.7 \text{ mg/g h}$ . In the provided optimum conditions, the occurrence of the denitrifying activity was also noticed. A large pH variation was registered (5–8.5) during treatment cycles. The granular activated algae system proved to be a promising alternative for wastewater treatment as it also sustains cost-efficient microalgae harvesting, with microalgae recovery efficiency ranging between 99.85 and 99.99% after granules settling with a velocity of  $19 \pm 3.6 \text{ m/h}$ .

**Key words** | activated algae granules, microalgae harvesting, settleability, wastewater treatment

## INTRODUCTION

Activated sludge systems are used widely for biological wastewater treatment (Zhang *et al.* 2014). However, as in the case of other applied alternative technologies for wastewater treatment, activated sludge-based processes are faced with several drawbacks. For instance, aeration processes are energy-intensive, requiring 60–65% from total energy costs related to wastewater treatment flow (Fernandez *et al.* 2011). Moreover, there are still problems globally with management of waste activated sludge, mainly due to the continuous increase of sludge production as a result of socio-economic systems development, high treatment costs, and legislative restrictions of sludge application (Guo *et al.* 2013). As a consequence, implementation of feasible, innovative technologies for wastewater treatment is encouraged. One of the proposed alternatives is represented by the use of the 'activated algae system', which is composed of bacteria and algae species developed in a symbiotic relationship (McGriff & McKinney 1972). This idea was sustained by researchers for decades due to the following reasons: no need for mechanical aeration, as oxygen is provided by algae through photosynthesis; simultaneous

removal of organic matter and nutrients; being sustainable in line with greenhouse gas mitigation strategies; and the possibility to decrease activated sludge production with simultaneous improvement of residual waste management, microalgae biomass being a well-known feedstock for a wide range of renewable resources (e.g., bioactive compounds and biofuels) (Mata *et al.* 2010; Su *et al.* 2012). Increasing interest in sustainable socio-ecological systems development, coupled with the potential benefits that can be obtained through valorization of the algae biomass, has resulted in a significant increase of research studies in this area (Chen *et al.* 2013; Wang *et al.* 2013).

Most of the representative algae species used for wastewater treatment processes have a microscopic cell size (usually less than  $30 \mu\text{m}$ ) (Wang *et al.* 2010). Unfortunately, this property has a great impact on scaling-up algae-based technology and on the economic feasibility of the biofuels production industry (Gonzalez-Fernandez & Ballesteros 2013). This is because the high costs required for microalgae harvesting, due to the low settling ability of the microalgae cells structures (usually lower than  $3.6 \times 10^{-3} \text{ m/h}$ )

O. Tiron

C. Bumbac (corresponding author)

I. V. Patroescu

V. R. Badescu

National Research and Development Institute for Industrial Ecology – ECOIND,  
71–73 Drumul Podu Dambovitei Street, 060652,  
Sector 6,  
Bucharest,  
Romania  
E-mail: costel.bumbac@incdecoind.ro

O. Tiron

C. Postolache

Department of Systems Ecology and Sustainability,  
Faculty of Biology,  
University of Bucharest,  
91–95 Splaiul Independentei Street, 050095,  
Sector 5,  
Bucharest,  
Romania

(Granados *et al.* 2012). Frequently applied microalgae harvesting techniques, such as centrifugation, chemical coagulation/flocculation, filtration, and gravity sedimentation, are faced with several drawbacks. Thus, high energy consumption and cost-inefficiency, risk of biomass contamination with metals, filters clogging, sensitivity to pH variation, etc. (Sun *et al.* 2013) are some of the reasons that highlight the necessity to develop an alternative, cost-efficient, and effective harvesting method. As a result, during recent years, other alternative harvesting methods were proposed, such as bio-flocculation using auto-flocculating microalgae species (Salim *et al.* 2011), microalgae pelletization using fungi (Zhou *et al.* 2013), microalgae separation using magnetic nanoparticles (Hu *et al.* 2014), etc. Research has continued in this area as no viable solution for use at industrial scale has been recognized until now.

Therefore, this study aimed to test a newly developed granular algae-based system for wastewater treatment, which also sustains the current strategy of the microalgae harvesting step. Activated algae granules were used for low-strength wastewater treatment with an emphasis on the following aspects: treatment performance recorded in terms of organic matter and nutrient removal; microalgae recovery efficiency from effluent after applying a single gravity sedimentation technique; and settleability of the activated algae biomass. Other objectives of the experimental work were to analyze the variations of the liquor's O<sub>2</sub> saturation and pH values during treatment cycles and the effect of pH variation on the activated algae granules' integrity.

## METHODS

### Activated algae inoculum

Activated algae inoculum was represented by floc structures composed of wild bacteria and microalgae species developed in symbiosis during pre-treated dairy wastewater treatment in laboratory conditions. Microalgae biomass was represented mainly by two morphological types: spherical and filamentous. Spherical microalgae were non-flocculating species of *Chlorella* characterized by small cell size (ranging between 1 and 8 µm in diameter), giving them poor settling ability (lower than  $5.4 \times 10^{-3}$  m/h).

### Granulation of the activated algae system

An activated algae system was used in previous research for wastewater treatment processes, mainly as floc structures

(Tricolici *et al.* 2014). For the present experiments, activated algae biomass was represented by granular entities developed in a photo-bioreactor (BIOSTAT® Bplus, Sartorius, Goettingen, Germany) with 1.5 L vessel volume. Biological inoculum used for granulation processes was represented by activated algae flocs. Feeding substrate was represented by 1 L of pre-treated dairy wastewater having the following chemical characteristics: chemical oxygen demand (COD) (100–400 mg O<sub>2</sub>/L), ammonium (NH<sub>4</sub><sup>+</sup>) (8.7–42 mg/L), nitrate (NO<sub>3</sub><sup>-</sup>) (<7 mg/L), nitrite (NO<sub>2</sub><sup>-</sup>) (<0.1 mg/L), phosphate (PO<sub>4</sub><sup>3-</sup>) (0.8–12 mg/L), magnesium (Mg<sup>2+</sup>) (7–35 mg/L), and calcium (Ca<sup>2+</sup>) (13–31 mg/L). The initial liquor's pH value ranged between 7 and 8. The granulation process was performed in sequencing batch mode, at high stirring speed (up to 150 rotations per minute (rpm)). Hydraulic retention time was decreased consecutively from 96 to 72, 48, and 24 h, depending on the time needed for almost complete COD and nutrient removal. This operational adjustment was conducted in order to ensure a continuous carbon supply and to avoid biomass starvation. Light was provided by an external cool-white lamp with 3,980 lm. At the outer wall of the bioreactor, light intensity was 235 µmol/m<sup>2</sup>/s. Photoperiodicity was set up to 15 h light–9 h dark, with the light cycle beginning immediately after photo-bioreactor feeding. At the end of each cultivation cycle, the stirring was stopped and the biomass was allowed to settle for 1 h. After biomass settling, the liquor was discharged, the settled biomass retained, and the bioreactor was fed with a new substrate.

### Experimental operation

The experiment consisted of treatment of low-strength wastewater in sequencing batch mode using activated algae granules and keeping the operational parameters and equipment applied for activated algae granulation processes, unless it is not specified otherwise. Each treatment cycle was conducted within 24 h via the following four steps: (1) bioreactor feeding with 1 L influent (15 min); (2) wastewater treatment (reaction step) at 120 rpm stirring speed (23 h 20 min); (3) stirring stopping and biomass settling for 15 min; (4) effluent withdrawal (10 min) followed by bioreactor feeding (1) with a new influent, while retaining the concentrated biomass. During the experiment, about 45 treatment cycles were carried out. Influent was obtained by mixing 140 mL of untreated and non-autoclaved strength dairy wastewater with 860 mL of distilled water and the following reagents: 45 mg/L NH<sub>4</sub>Cl, 100 mg/L MgSO<sub>4</sub>·7 H<sub>2</sub>O, 15 mg/L K<sub>2</sub>HPO<sub>4</sub>, and 30 mg/L CaCl<sub>2</sub>·2 H<sub>2</sub>O as supplementary sources of NH<sub>4</sub><sup>+</sup>,

Mg<sup>2+</sup>, PO<sub>4</sub><sup>3-</sup>, and Ca<sup>2+</sup>, respectively. As a result, the influent's organic matter and nutrient loadings varied in the following ranges: COD (70.4–211.2 mg O<sub>2</sub>/L), NH<sub>4</sub><sup>+</sup> (15.5–32.1 mg/L), NO<sub>3</sub><sup>-</sup> (<0.1 mg/L), NO<sub>2</sub><sup>-</sup> (<0.1 mg/L), PO<sub>4</sub><sup>3-</sup> (8.3–21.2 mg/L), Mg<sup>2+</sup> (13.8–34.1 mg/L), and Ca<sup>2+</sup> (26–38.7 mg/L). The initial biomass concentration was 1.1 g/L. The experiment was carried out in the absence of any aeration source, oxygen being provided during the light phase by the microalgae through photosynthesis. All interventions were performed using a special port with a diameter of 2.5 cm, which was closed during the reaction step in order to avoid external aeration.

### Microalgae recovery efficiency

Microalgae recovery efficiency from the effluent was determined based on the chlorophyll *a* concentration and using the following equation:

$$ME = [(Chla_I - Chla_F)/Chla_I] \times 100\% \quad (1)$$

where ME (%) is the microalgae recovery efficiency, Chla<sub>I</sub> (µg/L) is the chlorophyll *a* concentration of the entire biomass and Chla<sub>F</sub> (µg/L) is the chlorophyll *a* concentration of the effluent. The methods usually reported for microalgae recovery efficiency determination represent functions of the optical density of chlorophyll pigments read at a specific wavelength (Wang *et al.* 2010). However, in our case, granular structure, dense biomass and the presence of bacteria could affect chlorophyll's absorbance. Taking into consideration that chlorophyll *a* pigments can be found in all photosynthetic microalgae species (Paerl *et al.* 2003), we concluded that the measurement of the microalgae recovery efficiency as a function of chlorophyll *a* concentration will be the most appropriate option to ensure high accuracy of the results.

### Analytical methods

The COD indicator was analyzed according to the SR ISO 6060:1996 standard application method described in our previous research (Tricolici *et al.* 2014). Cations (NH<sub>4</sub><sup>+</sup>, Mg<sup>2+</sup>, Ca<sup>2+</sup>) and anions (NO<sub>3</sub><sup>-</sup>, NO<sub>2</sub><sup>-</sup>, PO<sub>4</sub><sup>3-</sup>) were determined according to SR EN ISO 14911:2003 and SR EN ISO 10304/1:2009 standards, respectively, and using DIONEX ion-chromatography system (Model ICS-3000, Sunnyvale, CA, USA). Chlorophyll *a* concentration from liquor was measured according to the SR ISO 10260:1996 standard. The liquor's pH and oxygen saturation (%) were determined continuously by built-in bioreactor electrode (Model Easy Ferm Plus K8

(200), Hamilton, Bonaduz, Switzerland) and sensor (Model OxyFerm FDA (225), Hamilton, Bonaduz, Switzerland), respectively. The indicators' analysis was performed at each third treatment cycle, with 15 treatment cycles being investigated overall. An additional four treatment cycles were conducted in order to determine the short-term effect of pH variation on the activated algae granules' integrity. In this case, the treatment cycles were maintained consecutively at four pH intervals: 5–5.5, 6–6.5, 7–7.5, and 8–8.5 using NaOH (1%), and H<sub>2</sub>SO<sub>4</sub> (1 N). Activated algae biomass (g/L) was analyzed as dry weight following the method described in our previous research (Tricolici *et al.* 2014). Diameter size of the activated algae granules and *Chlorella* sp. cells was determined using the Mastersizer 2000 analyzer (Malvern Instruments, Malvern, UK), with the particle refractive index being set to 1.060 (Aas 1996).

## RESULTS AND DISCUSSION

### Microalgae recovery efficiency and settleability of the activated algae granules

Under the pressure of stirring force, the microalgae filaments developed a dense, stable, and granular biological matrix (see Figure 1(a)) efficiently entrapping free microscopic algae cells from the liquor. As a result, it achieved a microalgae recovery efficiency ranging between 99.85 and 99.99%, and a chlorophyll *a* concentration in the effluent between 23 and 5.9 µg/L. This performance was obtained after applying the single gravity sedimentation harvesting technique, which is frequently used in activated sludge processes, and it is reported to be efficient only for the recovery of large algae cells (>70 µm) (Nurdogan & Oswald 1996). In Figure 1(a), activated algae granules are presented comparatively with activated algae flocs (Figure 1(b)) and activated algae granules (Figure 1(c)) after the settling step.

During the experiments, the granules' diameter size ranged between 600 and 1,900 µm, with the average size varying between 1,300 and 1,400 µm. This property, coupled with the dense biological matrix, determined a biomass settling velocity of 19 ± 3.6 m/h. This performance, along with the activated algae granules' diameter size, is comparable with that stated in the case of the aerobic granular sludge, Zheng *et al.* (2005) who reported a settling velocity for the aerobic granules of 18–31 m/h, with granule diameter sizes ranging between 500 and 1,200 µm. Besides stirring pressure and the presence of the filamentous microalgae, bacteria could represent another key factor of the

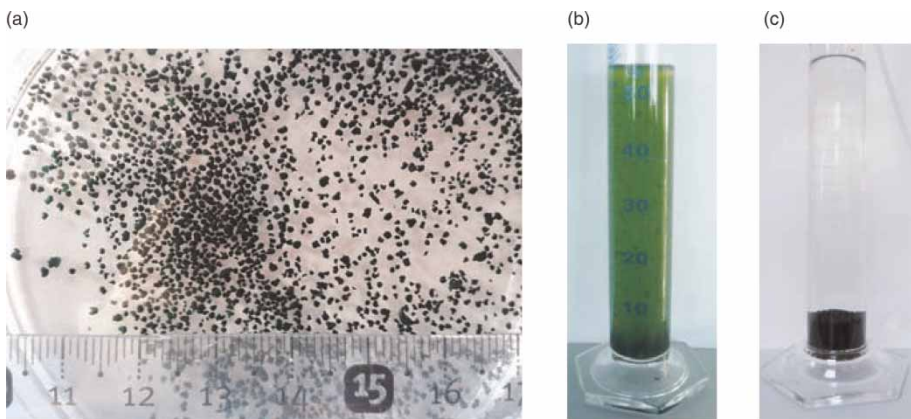


**Figure 1** | Images of the activated algae granules (a), settled activated algae flocs (note poor settleability of free *Chlorella* sp. cells remaining in the liquor) (b), and settled activated algae granules (note clear effluent resulting after biomass settling) (c).

granules' development, integrity, and settleability performance. For instance, *de Godos et al.* (2014) recently reported a good settling velocity (0.28–0.42 m/h) achieved after mixing activated sludge with microalgae biomass.

### O<sub>2</sub>% variation during wastewater treatment

Two types of patterns were recorded in the case of O<sub>2</sub>% variation, each of them being composed by several levels. An example of the first pattern (Pattern I), which was mainly representative for the first half of the conducted wastewater treatment cycles, is represented in *Figure 2(a)*. In this case the pattern followed three levels:

- (1) The first level started immediately after the photobioreactor feeding and it was characterized by the maintenance of O<sub>2</sub>% between 0 and 1%, most probably due to the fact that the oxygen supply provided by the microalgae during photosynthesis was similar to the oxygen uptake rate required for the biochemical oxidation processes. The duration of this level was directly correlated with the COD load (see *Figure 2(a)* in comparison with *Figure 2(b)*).
- (2) The second level was highlighted by a fast increase of O<sub>2</sub>%, even exceeding 100%. It is important to point out that this level started after almost complete COD removal, being a sign of the low organic matter concentration in the liquor (<30 mg O<sub>2</sub>/L). For instance, in the case of *Figure 2(a)*, at the moment of O<sub>2</sub>% increase, the COD concentration in the liquor was 4.4 mg O<sub>2</sub>/L. During this level, at a certain time, a decrease of O<sub>2</sub>% was noticed (without decreasing below 80%), as shown in *Figure 2(a)* and *2(b)*. This effect could be caused by the occurrence of photorespiration processes (*Moroney*

*et al.* 2013) as a result of microalgae maintenance at high O<sub>2</sub>% and low CO<sub>2</sub> supply (due to the low availability of organic matter).

- (3) The third level started simultaneously with the system entering the dark cycle and it was characterized by the decrease of O<sub>2</sub>% to about 0%.

An example of the second pattern of O<sub>2</sub>% variation (Pattern II) is represented in *Figure 2(c)*. As can be seen, Pattern II is differentiated from Pattern I by the following aspects:

- (1) maintenance of O<sub>2</sub>% in the first level to 0%;
- (2) appearance of the additional level of O<sub>2</sub>% variation, characterized by a slow increase of O<sub>2</sub>% after maintenance of the indicator's value to 0%;
- (3) no decrease of O<sub>2</sub>% saturation was noticed after the indicator's value increase above 100%.

This type of pattern was representative for the second half of the performed wastewater treatment cycles and was recorded after the biomass concentration more than doubled (from 1.1 to 2.4 g/L). Therefore, we assumed that in the case of this pattern, oxygen provided through photosynthetic processes was lower than that used for organic matter degradation, possibly due to the decrease of the oxygen production rate as a result of the shadow effect caused by the increase of biomass concentration. The longer duration of the first level of the pattern at a lower initial COD loading (see *Figure 2(c)* in comparison with *Figure 2(a)*) sustains the above-mentioned hypothesis.

In *Figure 2(d)* the variations of COD, NH<sub>4</sub><sup>+</sup>, NO<sub>2</sub><sup>-</sup>, and NO<sub>3</sub><sup>-</sup> related to Pattern II are represented. Thus, it can be seen that the increase of NO<sub>3</sub><sup>-</sup> concentration in the liquor, with the simultaneous decrease of NH<sub>4</sub><sup>+</sup> concentration and

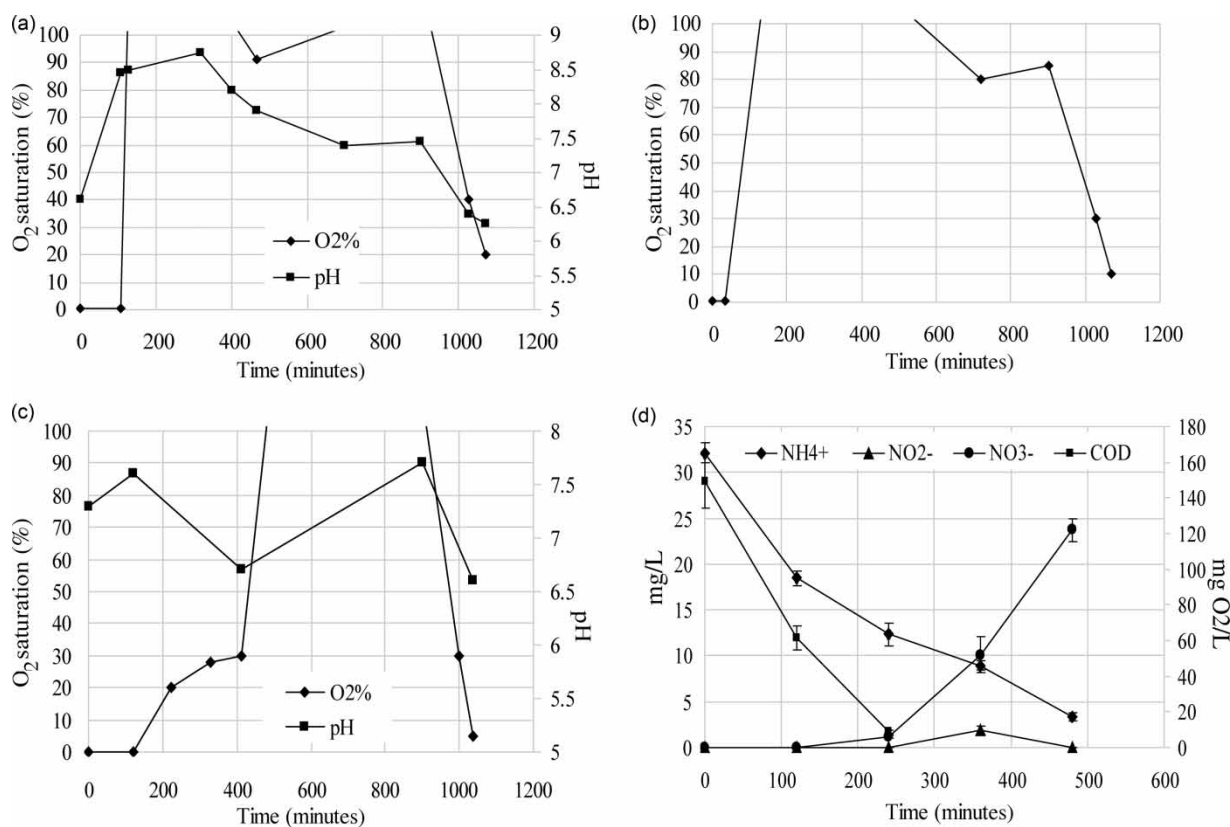


**Figure 2** | Time variations of the O<sub>2</sub>% and pH during the light phase of the wastewater treatment cycles relating to COD concentration in the influent and the NO<sub>3</sub><sup>-</sup> concentration in the effluent: (a) 211.2 mg O<sub>2</sub>/L COD, 43.2 mg/L NO<sub>3</sub><sup>-</sup> (Pattern I); (b) 96.8 mg O<sub>2</sub>/L COD, 51.1 mg/L NO<sub>3</sub><sup>-</sup> (Pattern I); (c) 149.6 mg O<sub>2</sub>/L COD, 63.2 mg/L NO<sub>3</sub><sup>-</sup> (Pattern II); (d) the variation of COD, NH<sub>4</sub><sup>+</sup>, NO<sub>2</sub><sup>-</sup> and NO<sub>3</sub><sup>-</sup> recorded during O<sub>2</sub>% variation represented in Figure 2(c).

the increase of O<sub>2</sub>%, clearly emphasizes the occurrence of the nitrification processes. Taking into account that the fast increase of O<sub>2</sub>% started after almost complete NH<sub>4</sub><sup>+</sup> removal from the liquor, we assumed that the lower rate of O<sub>2</sub> production and the occurrence of the intensive nitrification processes, along with the increase of O<sub>2</sub>% from 0%, could also explain the initial slow increase of O<sub>2</sub>%.

Owing to the slower increase of O<sub>2</sub>%, biomass maintenance at an O<sub>2</sub>% value higher than 100% was shorter in comparison with Pattern I. As a result, no decrease of O<sub>2</sub>% was recorded until the system entered the dark phase.

### pH variation during wastewater treatment

During the investigated wastewater treatment cycles, the pH indicator varied in a wide interval: 5–8.5. Moreover, as in the case of the O<sub>2</sub>% indicator, two types of pattern (Pattern I, Pattern II) were recorded for pH variation, represented in Figure 2(a) and 2(c), respectively, which correlated with O<sub>2</sub>% patterns. Thus, in the case of Pattern I (Figure 2(a)) the pH indicator followed a continuous increase until the

O<sub>2</sub>% started to decrease. This trend could be caused by CO<sub>2</sub> and HCO<sub>3</sub><sup>-</sup> consumption by photoautotrophic microalgae and implicitly by OH<sup>-</sup> accumulation in the liquor (Markou & Georgakakis 2011). On the contrary, the decrease of pH value with the O<sub>2</sub>% decrease could relate to the occurrence of photorespiration processes (as mentioned previously) or with a lack of inorganic carbon sources as a result of almost complete COD removal during even the first hours of the treatment cycles.

In comparison with Pattern I, the Pattern II (Figure 2(c)) pH followed a decreasing trend with the increase of O<sub>2</sub>%. Taking into account the increase of the NO<sub>3</sub><sup>-</sup> concentration during this level, we assumed that the intensive nitrification process began to dominate the metabolic activity of the microalgae causing the pH decrease. The pH started to increase again after almost complete nitrification, which correlated with the fast increase of O<sub>2</sub>% (Figure 2(c) and 2(d)). As in the case of Pattern I, the pH started to decrease simultaneously with the biomass entering the dark cycle. It is important to emphasize that wastewater dilution could have highly influenced pH variation. Thus, a narrower

variation of pH value during the treatment of undiluted dairy wastewater could be anticipated.

### Influence of pH variation on granules' integrity

The wide variation of pH values highlighted the necessity to investigate whether the indicator's value has an influence on the activated algae granules' integrity and implicitly on the microalgae recovery efficiency. Thus, after consecutive increases of the pH value from 5 to 8.5, no significant differences between size distribution of the activated algae granules were recorded, with the granules' average diameter size being 1,341.5, 1,334.9, 1,339, and 1,346  $\mu\text{m}$  related to the pH interval of 5–5.5, 6–6.5, 7–7.5, and 8–8.5, respectively (Annex 1, available online at <http://www.iwaponline.com/wst/071/010.pdf>). Moreover, the residual chlorophyll *a* concentration in effluents related to pH intervals of 5–5.5, 6–6.5, and 7–7.5 was 5.9  $\mu\text{g/L}$ ; in the case of the pH interval of 8–8.5, the indicator's value increased to 7.9  $\mu\text{g/L}$ . As a result, in all applied pH intervals, microalgae recovery efficiency was maintained at 99.98%. Therefore, the variation of the liquor's pH value between 5 and 8.5, for a short period of time (about 24 h), did not affect granular structure. However, further studies will be necessary to identify long-term effects.

### COD and nutrient removal

COD concentration in effluent ranged between 4.4 and 26.4 mg  $\text{O}_2/\text{L}$  being removed with an efficiency of 86.4–97.9%. It was noticed that the above-reported results were recorded within the first hours after photo-bioreactor feeding, until the increase of  $\text{O}_2\%$  from (about) 0% (as mentioned previously). During this period, the COD removal rate was  $17.4 \pm 3.9$  mg  $\text{O}_2/\text{g h}$ . An example of the COD concentration evolution during the treatment cycle is represented in Figure 3(a).

After monitoring the variation of  $\text{NH}_4^+$  concentration in liquor during the light cycle, it was found that 53–74% of nutrient concentration was consumed by the biomass until almost complete COD removal ( $<10$  mg  $\text{O}_2/\text{L}$ ) was achieved (an example is provided in Figure 3). During this time, the nutrient removal rate was  $1.8 \pm 0.6$  mg/g h. With the beginning of the  $\text{O}_2\%$  increase from (about) 0%, the remaining  $\text{NH}_4^+$  concentration in the liquor was mainly involved in nitrification processes, with the indicator's concentration in the effluent being below 0.1 mg/L. As a result,  $\text{NO}_3^-$  was detected in effluents, at concentrations varying between 18.9 and 63.2 mg/L, mainly depending on the initial  $\text{NH}_4^+$  load. It was noticed that complete nitrification

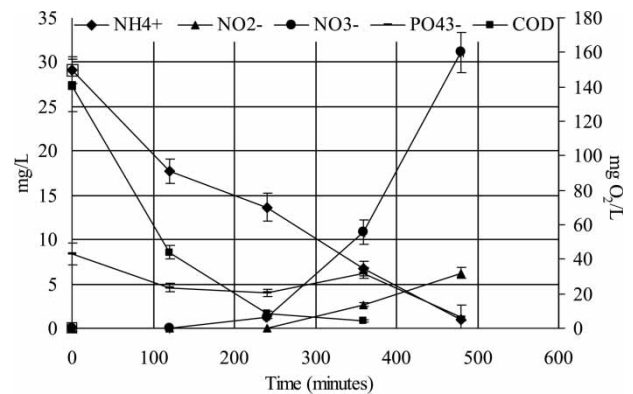


Figure 3 | Variation of COD,  $\text{NH}_4^+$ ,  $\text{NO}_2^-$ ,  $\text{NO}_3^-$  and  $\text{PO}_4^{3-}$  during the light cycle.

was achieved generally within the first 8 h of the wastewater treatment cycle, during which time the rate of  $\text{NH}_4^+$  transformation to  $\text{NO}_3^-$  increased, with the increase of  $\text{O}_2\%$ , from  $0.14 \pm 0.05$  to  $1.5 \pm 0.4$  mg  $\text{NH}_4^+/\text{g h}$ . During the experiments,  $\text{NH}_4^+$  removal through ammonia volatilization could be considered negligible since the pH indicator's value did not exceed 8.5 (de Godos et al. 2009).

Activated algae granules were characterized by dense biological structure, a property that can favor the development of denitrifying bacteria, as it is usually achieved in the case of aerobic granular sludge development (Yilmaz et al. 2007). Moreover, the maintenance of  $\text{O}_2\%$  to (about) 0% during the first level of the  $\text{O}_2\%$  variation pattern and the low value of the indicator during the dark cycle could also promote the development of denitrifying bacteria. As a result, an additional test was conducted in order to evaluate the presence of denitrifying activity. After 8 h of treatment (when almost complete nitrification occurs), 100 mL of undiluted dairy wastewater were added to the liquor in order to decrease the  $\text{O}_2\%$  to 0% and to provide the supplementary carbon source required for denitrification processes. Sixteen hours after fresh wastewater addition, the  $\text{NO}_3^-$  concentration from the liquor decreased from 25 to 1.3 mg/L, thus emphasizing the occurrence of denitrifying activity. Taking into account the recorded results, it could be assumed that, besides  $\text{NH}_4^+$  assimilation, nitrification with simultaneous denitrification processes could have occurred in the first level and/or at the beginning of the second level of the  $\text{O}_2\%$  variation pattern.

In the case of  $\text{NO}_2^-$  concentration, a slight increase was registered, along with the increase of  $\text{O}_2\%$ , during intensive nitrification processes (Figure 3). However, at the end of the cycles, the residual concentration of the parameter was below 0.1 mg/L.

$\text{PO}_4^{3-}$  removal efficiency varied in a wide interval: 11.2–84.9%. A decreasing trend of  $\text{PO}_4^{3-}$  concentration was noticed especially during the first 2–4 h of the wastewater treatment cycle, when the indicator's rate was  $1.3 \pm 0.7 \text{ mg PO}_4^{3-}/\text{g h}$ . In this case, there are two possible methods for the removal of biological phosphorus from liquor: assimilation and excess accumulation in the cells through a 'luxury uptake' storage mechanism. Moreover, the increase of the pH value above 8 could also have promoted the increase of the  $\text{PO}_4^{3-}$  removal rate through adsorption on the aggregated algae cells (Zhou *et al.* 2012). Phosphorus removal through precipitation could be considered negligible due to the fact that the pH did not exceed the value of 9 (de Godos *et al.* 2009). In some cases, an increase of a nutrient's concentration in the liquor was recorded (as shown in Figure 3) after almost complete COD removal. Thus, catabolic reactions of the aerobic organic matter degradation strongly decreased at that time. As a result,  $\text{PO}_4^{3-}$  release from cells could have occurred after being involved in the energy generation reactions required to conduct cell processes.

## CONCLUSIONS

The current study tested the efficiency of using granular activated algae for wastewater treatment. The experimental results showed that the novel proposed biological system proved to be a feasible alternative for simultaneously removing organic matter and nutrients from wastewater in the absence of mechanical aeration systems, using only the oxygen provided by microalgae through photosynthesis. Granular activated algae and the provided operational conditions also favored the development of denitrifying taxa, results that should be taken into consideration for further studies. Moreover, the use of activated algae granules proved to have several advantages besides the activated algae flocs: it significantly improves the activated algae settleability; ensures almost complete recovery of the microscopic algae from effluent; and sustains the use of microscopic algae species (with poor settling ability) for wastewater treatment without additional costs for microalgae recovery and adjustment of operational conditions in the harvesting step.

## ACKNOWLEDGEMENTS

This study was undertaken within the Nucleu Project (PN 09 13 03 12), supported by the Romanian Ministry of

National Education – State Authority for Scientific Research, Technological Development and Innovation.

## REFERENCES

- Aas, E. 1996 Refractive index of phytoplankton derived from its metabolite composition. *Journal of Plankton Research* **18** (12), 2223–2249.
- Chen, L., Wei, J., Wanh, W. & Wang, C. 2013 Combination of microalgae cultivation with membrane processes for the treatment of municipal wastewater. *Water Science and Technology* **68** (11), 2374–2381.
- de Godos, I., Blanco, S., Garcia-Encina, A. P., Becares, E. & Munoz, R. 2009 Long-term operation of high rate algal ponds for the bioremediation of piggery wastewaters at high loading rates. *Bioresource Technology* **100**, 4332–4339.
- de Godos, I., Vargas, V. A., Guzman, H. O., Soto, R., Garcia, B., Garcia, P. A. & Munoz, R. 2014 Assessing carbon and nitrogen removal in a novel anoxic-aerobic cyanobacterial-bacterial photobioreactor configuration with enhanced biomass settleability. *Water Research* **61**, 77–85.
- Fernandez, J. F., Castro, C. M., Rodrigo, A. M. & Canizares, P. 2011 Reduction of aeration costs by tuning a multi-set point on/off controller: a case study. *Control Engineering Practice* **19** (10), 1231–1237.
- Gonzalez-Fernandez, C. & Ballesteros, M. 2013 Microalgae auto-flocculation: an alternative to high energy consuming harvesting methods. *Journal of Applied Phycology* **25** (4), 991–999.
- Granados, M. R., Acien, F. G., Gomez, C., Fernandez-Sevilla, J. M. & Grima Molina, E. 2012 Evaluation of flocculants for the recovery of freshwater microalgae. *Bioresource Technology* **118**, 102–110.
- Guo, W.-Q., Yang, S.-S., Xiang, W.-S., Wang, X.-J. & Ren, N.-Qi 2013 Minimization of excess sludge production by in-situ activated sludge treatment processes – a comprehensive review. *Biotechnology Advances* **31** (8), 1386–1396.
- Hu, Y.-R., Guo, C., Wang, F., Wang, S.-K., Pan, F. & Liu, C.-Z. 2014 Improvement of microalgae harvesting by magnetic nanocomposites coated with polyethylenimine. *Chemical Engineering Journal* **242**, 341–347.
- Markou, G. & Georgakakis, D. 2011 Cultivation of filamentous cyanobacteria (blue-green algae) in agro-industrial wastes and wastewaters: a review. *Applied Energy* **88** (10), 3389–3401.
- Mata, T. M., Martins, A. A. & Caetano, N. S. 2010 Microalgae for biodiesel production and other applications: a review. *Renewable and Sustainable Energy Reviews* **14** (1), 217–232.
- McGriff, C. E. & McKinney, E. R. 1972 The removal of nutrients and organics by activated algae. *Water Research* **6** (10), 1155–1164.
- Moroney, V. J., Jungnick, N., DiMario, J. R. & Longstreth, J. D. 2013 Photorespiration and carbon concentrating mechanisms: two adaptations to high  $\text{O}_2$ , low  $\text{CO}_2$  conditions. *Photosynthesis Research* **117**, 121–131.

- Nurdogan, Y. & Oswald, W. J. 1996 Tube settling of high rate pond algae. *Water Science and Technology* **33** (7), 229–241.
- Paerl, H. W., Valdes, L. M., Pinckney, J. L., Piehler, M. F., Dyble, J. & Moisander, P. H. 2003 Phytoplankton photopigments as indicators of estuarine and coastal eutrophication. *Bioscience* **53** (10), 953–964.
- Salim, S., Bosma, R., Vermue, H. M. & Wijffels, H. R. 2011 Harvesting of microalgae by bio-flocculation. *Journal of Applied Phycology* **23** (5), 849–855.
- SR EN ISO 10304/1 2009 Water quality – Determination of dissolved anions by liquid chromatography of ions (Part I). Determination of bromide, chloride, fluoride, nitrate, nitrite, phosphate and sulfate. Romanian Standards Association, Bucharest, Romania.
- SR EN ISO 14911 2003 Water quality – Determination of dissolved  $\text{Li}^+$ ,  $\text{Na}^+$ ,  $\text{NH}_4^+$ ,  $\text{K}^+$ ,  $\text{Mn}^{2+}$ ,  $\text{Ca}^{2+}$ ,  $\text{Mg}^{2+}$ ,  $\text{Sr}^{2+}$  and  $\text{Ba}^{2+}$  using ion chromatography. Method for Water and Wastewater. Romanian Standards Association, Bucharest, Romania.
- SR ISO 6060 1996 Water quality – Determination of the chemical oxygen demand. Romanian Standards Association, Bucharest, Romania.
- SR ISO 10260 1996 Water quality – Measurement of biochemical parameters – Spectrometric determination of the chlorophyll *a* concentration. Romanian Standards Association, Bucharest, Romania.
- Su, Y., Mennerich, A. & Urban, B. 2012 Synergistic cooperation between wastewater-born algae and activated sludge for wastewater treatment: influence of algae and sludge inoculation ratios. *Bioresource Technology* **105**, 67–73.
- Sun, X., Wang, C., Tong, Y., Wang, W. & Wei, J. 2013 A comparative study of microfiltration and ultrafiltration for algae harvesting. *Algal Research* **2** (4), 437–444.
- Tricolici, O., Bumbac, C., Patroescu, V. & Postolache, C. 2014 Dairy wastewater treatment using an activated sludge-microalgae system at different light intensities. *Water Science and Technology* **69** (8), 1598–1605.
- Wang, L., Min, M., Li, Y., Chen, P., Chen, Y., Liu, Y., Wang, Y. & Ruan, R. 2010 Cultivation of green algae *Chlorella* sp. in different wastewaters from municipal wastewater treatment plant. *Applied Biochemistry and Biotechnology* **162** (4), 1174–1186.
- Wang, H., Hu, Z., Xiao, Bo, Cheng, Q. & Li, F. 2013 Ammonium nitrogen removal in batch cultures treating digested piggery wastewater with microalgae *Oedogonium* sp. *Water Science and Technology* **68** (2), 269–275.
- Yilmaz, G., Lemaire, R., Keller, J. & Yuan, Z. 2007 Simultaneous nitrification, denitrification, and phosphorus removal from nutrient-rich industrial wastewater using granular sludge. *Biotechnology and Bioengineering* **100** (3), 529–541.
- Zhang, X., Li, X., Zhang, Q., Peng, Q., Zhang, W. & Gao, F. 2014 New insight into the biological treatment by activated sludge: the role of adsorption process. *Bioresource Technology* **153**, 160–164.
- Zheng, Yu-M., Yu, H.-Q. & Sheng, G.-P. 2005 Physical and chemical characteristics of granular activated sludge from a sequencing batch airlift reactor. *Process Biochemistry* **40** (2), 645–650.
- Zhou, W., Min, M., Li, Y., Hu, B., Ma, X., Cheng, Y. & Liu, Y. 2012 A hetero-photoautotrophic two-stage cultivation process to improve wastewater nutrient removal and enhance algal lipid accumulation. *Bioresource Technology* **110**, 448–455.
- Zhou, W., Min, M., Hu, B., Ma, X., Liu, Y., Wang, Q., Shi, J., Chen, P. & Ruan, R. 2013 Filamentous fungi assisted bio-flocculation: a novel alternative technique for harvesting heterotrophic and autotrophic microalgal cells. *Separation and Purification Technology* **107**, 158–165.

First received 22 August 2014; accepted in revised form 23 December 2014. Available online 14 January 2015